PHYSICAL REVIEW C, VOLUME 60, 031603

Signature of geometrical effects in heavy-ion reactions below 100 MeV/nucleon

F. Haddad,[1] Ph. Eudes,[1] Z. Basrak,[2] and F. Sébille[1]
[1]*Laboratoire SUBATECH, 4 Avenue A. Kastler, F-44 072 Nantes Cedex 03, France*
[2]*Ruder Bošković Institute, HR-10 001 Zagreb, Croatia*
(Received 8 June 1999; published 23 August 1999)

An extensive study of dynamically emitted charged particles was carried out within the framework of a semiclassical transport model. Several systems having different total mass and asymmetry were studied over a wide range of incident energies. It was found that dynamical emission occurring in heavy-ion collisions is the signature of a smooth transition between the low-energy reaction mechanism (deep inelastic model) and the high-energy reaction mechanism (participant-spectator model). [S0556-2813(99)50809-1]

PACS number(s): 25.70.−z, 24.10.Cn

When studying heavy-ion collisions, it is currently admitted that deep inelastic collisions are the dominant mechanism at low incident energy (a few ten MeV/nucleon) and that above a few hundred MeV/nucleon a participant-spectator picture of the collision is meaningful [1]. At intermediate energies, between 30 MeV/nucleon and about a hundred MeV/nucleon, recent experimental works have shown that the binary dissipative collision (BDC) is the main reaction mechanism [2–8]. In most of these experimental studies, the BDC is considered a two-stage process. During the first stage of the reaction, the projectile and the target interact mutually strongly and out-of-equilibrium emission occurs. The second stage of the collision starts with the formation of two excited outgoing fragments labeled as the quasiprojectile (QP) and the quasitarget (QT). These heavy fragments are supposed to be thermalized and hence they decay by statistical emission of neutrons, light charged particles, and also intermediate-mass fragments (IMF). To derive the properties of hot nuclei formed during the BDC's, one has to assume that it is possible to discriminate the products of the dynamical stage from the products of the statistical stage. From such studies, very high excitation energies (well above the binding energy, i.e., ~8 MeV/nucleon) and temperatures (over 10 MeV) have been reported for different systems and incident energies (see Ref. [9] and references therein).

However, the separation of the two regimes of the BDC, namely, the dynamical from the statistical, is not an easy task. In a recent paper, Eudes *et al.* have demonstrated the crucial role of the dynamics in heavy-ion reactions at intermediate energies [9]. The authors have used the time evolution of particle emission to determine a characteristic time that allows the separation of the dynamical contribution from the statistical one [9,10]. Using this criterion, one obtains a copious particle emission at the first collision stage. These promptly emitted particles are present over the whole rapidity spectrum, although they dominate the midrapidity region. Such an important contribution at midrapidity has recently been reported in several experimental papers for light [11,12] and heavy systems [5,13,14]. Łukasik and the INDRA Collaboration have also reported a large midrapidity emission that cannot be explained by the subsequent statistical emission of the QP and the QT [4]. This promptly emitted component dominates central collisions: for the Ar+Al system at 65 MeV/nucleon it amounts to 50% of the total particle emission [9]. It comprises the common and weak preequilibrium emission. In the following we label this component DE (as dynamical emission). DE affects the excitation energy and the temperature that a nucleus is supposed to reach [15]. In a recent paper, D. Doré *et al.* [16] have shown that without correctly taking into account this contribution, one overestimates the excitation energy reached in central Ar+Ni collisions by a factor of 1.8.

The present study has been performed within the framework of the Landau-Vlasov microscopic model in direct connection with the recent results of Eudes *et al.* [9]. We have studied five systems (^{40}Ar+^{27}Al, ^{40}Ar+^{107}Ag, ^{107}Ag+^{40}Ar, ^{36}Ar+^{58}Ni, and ^{120}Xe+^{129}Sn) covering a large variety of total mass and asymmetry over a wide incident energy range (from 40 to 100 MeV/nucleon). After a brief sketch of the model used, a theoretical estimate of the DE occurring in heavy-ion collisions at intermediate energies is made together with a comparison with existing experimental data. It is shown that DE is a dominant way of evacuating the available energy in central heavy-ion collisions. Consequently, DE is a key quantity in understanding the heavy-ion collision history, especially if thermodynamical quantities are examined.

Let us briefly describe the main features of the model used, the Landau-Vlasov model [17]. It solves numerically the Landau-Vlasov equation which describes the evolution of the one-body phase-space distribution function $f(\mathbf{r},\mathbf{p};t)$:

$$\frac{\partial f(\mathbf{r},\mathbf{p};t)}{\partial t}+\{f(\mathbf{r},\mathbf{p};t),H\}=I_{\mathrm{coll}}(f(\mathbf{r},\mathbf{p};t)), \tag{1}$$

where $\{\,,\}$ stands for the Poisson brackets, H is the one-body mean-field Hamiltonian, and $I_{\mathrm{coll}}(f(\mathbf{r},\mathbf{p};t))$ is the two-body collision integral based on the Uehling-Uhlenbeck approximation.

This collision term reads

$$\begin{aligned} I_{\mathrm{coll}}=\frac{g}{4m^2}\frac{1}{\pi^3\hbar^3}\int d\mathbf{p_2}\,d\mathbf{p_3}\,d\mathbf{p_4}\frac{d\sigma_{NN}}{d\Omega}\,\delta(\mathbf{p}+\mathbf{p_2}-\mathbf{p_3}-\mathbf{p_4}) \\ \times\delta(\epsilon+\epsilon_2-\epsilon_3-\epsilon_4)[(1-\overline{f})(1-\overline{f_2})f_3f_4 \\ -(1-\overline{f_3})(1-\overline{f_4})f_2f], \end{aligned} \tag{2}$$

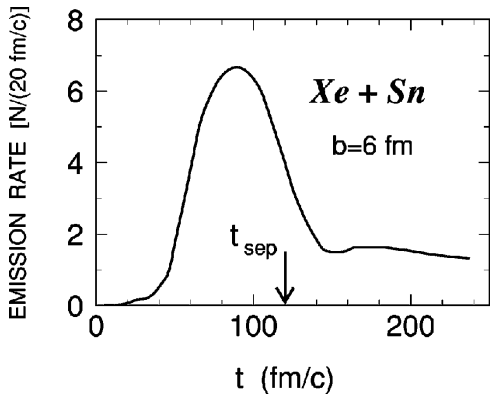

FIG. 1. Time evolution of the particle emission rate for the Xe+Sn reaction at 50 MeV/nucleon and $b=6$ fm.

where $\bar{f}=[(2\pi\hbar)^3/g]f(\mathbf{r},\mathbf{p};t)$ is the occupation number, g is the degeneracy, m is the nucleon mass, and σ_{NN} is the nucleon-nucleon (NN) cross section.

The momentum-dependent Gogny interaction $D1$-$G1$ ($K_\infty=228$ MeV) [18] has been used to describe the mean-field potential. In spite of intensive theoretical studies, in-medium effects on the NN cross section σ_{NN} remain an open problem [19]. Therefore, the isospin- and energy-dependent free-scattering value of σ_{NN} have been implemented in our model. This set of physically grounded parameters has already allowed, among other studies, a successful description of the flow of nuclear matter [20,21] and of the linear momentum transfer in heavy-ion reactions [22].

In heavy-ion collisions at intermediate energies, the emission process is characterized by a complex time evolution. A typical time evolution is shown in Fig. 1 for charged particles of the Xe+Sn reaction at 50 MeV/nucleon and $b=6$ fm. The emission starts shortly after the contact ($\simeq 0$ fm/c) and reaches a maximum after $t=80$ fm/c, then decreases and stabilizes. The characteristic time which allows us to separate the two regimes of emission is labeled $t_{\rm sep}$. It is the time at which the system breaks into a QT and a QP and it is known up to the value of the time step by which the system phase space is recorded; typically, 10 fm/c. For the system considered in Fig. 1, $t_{\rm sep}$ is equal to 120 fm/c. At a given energy, $t_{\rm sep}$ increases with decreasing impact parameter [9]. On the one hand, particles emitted before $t_{\rm sep}$ clearly originate from the overlapping zone of the target and the projectile and have an anisotropic distribution [9] which is similar to the behavior of the participant emission observed at higher incident energy. The system evolves rapidly and corresponds to a compact dinuclear shape which emits *mostly* at midrapidity. This type of emission has been claimed in Xe+Sn at 50 MeV/nucleon [23]. On the other hand, particles emitted after $t_{\rm sep}$ show a pattern characteristic of an evaporation process coming from the two excited outgoing heavy fragments. Thus, we label charged particles emitted before $t_{\rm sep}$ as dynamical emission.

In order to extend the work initiated in Ref. [9], DE is studied for various systems having different size and asymmetry. To facilitate the comparison, we define the quantity

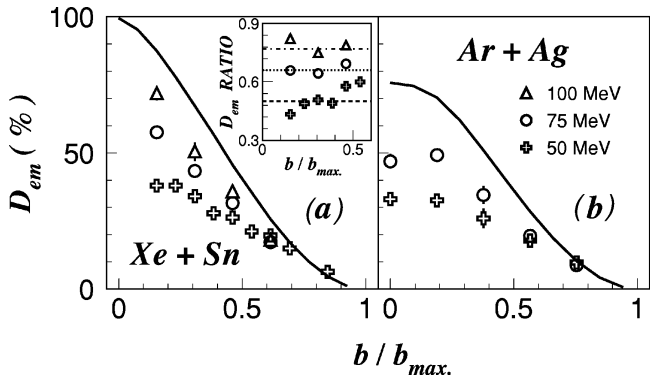

FIG. 2. Simulation results for the evolution of dynamical emission as a function of the reduced impact parameter (a) for the symmetric Xe+Sn system at 50, 75, and 100 MeV/nucleon incident energies and (b) for the asymmetric Ar+Ag system at 50 and 75 MeV/nucleon incident energies. The inset displays the ratio between $D_{\rm em}$ and the expected participant contribution in a pure geometrical assumption (solid curve).

$$D_{\rm em}=100\,\frac{\text{No. of DE}}{Z_{\rm tot}}, \tag{3}$$

which corresponds to the amount of charged particles emitted before $t_{\rm sep}$ divided by the total charge of the system, $Z_{\rm tot}=Z_{\rm T}+Z_{\rm P}$. $D_{\rm em}$ takes value 0% if no DE occurs, and 100% if the whole system disintegrates by DE.

Figure 2(a) displays $D_{\rm em}$ for the quasisymmetric ^{129}Xe $+\,^{120}$Sn system as a function of the centrality of the reaction for three different incident energies. As a reference, shown is a curve that represents the size of the overlapping region between the target and the projectile in a fully geometrical assumption. The centrality of the reaction is expressed via the reduced impact parameter (RIP), i.e., the impact parameter normalized according to $b_{\rm max}=R_{\rm T}+R_{\rm P}$, where $R_{\rm T}$ ($R_{\rm P}$) stands for the radius of the target (projectile). The values and the error bars reported in the figure correspond, respectively, to the mean value and the difference obtained by considering DE at $t_{\rm sep}$ and at $t_{\rm sep}+10$ fm/c. At 50 MeV/nucleon (crosses), $D_{\rm em}$ increases with increasing centrality. In peripheral collisions, however, its value is closer to the percentage of matter present in the overlap of the target and the projectile. As the RIP decreases, $D_{\rm em}$ starts to deviate from this pure geometrical assumption and saturates around 40% for $b/b_{\rm max}<0.3$. As the incident energy increases to 75 MeV/nucleon (circles), the qualitative behavior of $D_{\rm em}$ is similar to that obtained at 50 MeV/nucleon, but the global trend of the data is closer to that of the simple geometrical assumption. Indeed, saturation appears for smaller values of the RIP ($\simeq 0.2$) and reaches 60% of the $Z_{\rm tot}$. At an incident energy of 100 MeV/nucleon (triangles), $D_{\rm em}$ is still closer to the geometrical case, reaching up to 80% of the $Z_{\rm tot}$ in central collisions.

An interesting feature displays the ratio of $D_{\rm em}$ and the corresponding value of the geometrical-assumption curve at the same RIP [see inset on Fig. 2(a)]. As discussed above, this ratio is close to unity in peripheral collisions. Its value decreases with centrality and displays quite constant behav-

TABLE I. List of systems and incident energies studied in head-on collisions.

System	Incident energy (MeV/nucleon)
^{40}Ar+^{27}Al	41, 65
^{40}Ar+^{107}Ag	50, 75, 100
^{107}Ag+^{40}Ar	50
^{36}Ar+^{58}Ni	52, 74, 95
^{120}Xe+^{129}Sn	50, 75, 100

ior for RIP$<$0.6. At 50 MeV/nucleon (dashed line), this constant value is equal to 0.5 and increases with increasing incident energy, reaching 0.67 at 75 MeV/nucleon (dotted line) and almost 0.8 at 100 MeV/nucleon (dash-dotted line).

Figure 2(b) displays the DE obtained for the asymmetric Ar+Ag system as a function of the RIP. As in Fig. 2(a), the curve represents the value of a simple geometrical assumption for this asymmetric system. $D_{\rm em}$ evolves similarly to the Xe+Sn case. Peripheral-collision values are compatible with the geometrical assumption and $D_{\rm em}$ increases with increasing centrality of the collision. It finally saturates for the most central collision. $D_{\rm em}$ is larger at 75 MeV/nucleon (circles) than at 50 MeV/nucleon (crosses), but remains below the estimate of the geometrical model. For this system, the constant value of the above defined ratio for central collisions is equal to 0.68 at 75 MeV/nucleon and to 0.46 at 50 MeV/nucleon.

Additional calculations have been made for a large variety of systems and energies (see Table I for a review). Some of these systems, such as Ar+Ni, have been measured experimentally by the INDRA Collaboration [11]. It is interesting to compare their experimental findings with our calculations. Figure 3 shows the DE as a function of centrality for the Ar+Ni reaction. The comparison is made for three different incident energies over the whole impact parameter range. The points correspond to the simulation, whereas the hatched area represents the domain of experimental results. This domain is delimited by the two slightly different results obtained using two distinct methods for extracting DE. At 52 MeV/nucleon, a large difference exists in central collisions between the results of the two experimental methods, which is almost negligible in peripheral collisions. As the incident energy increases, the two methods converge. Overall good

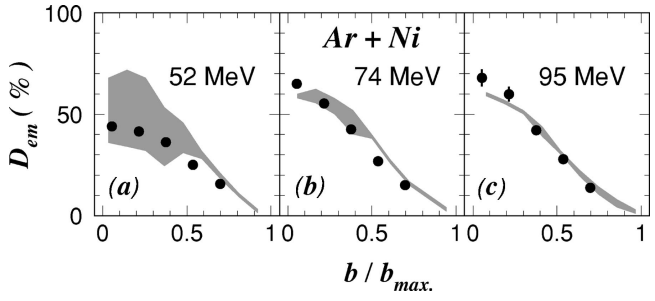

FIG. 3. Comparison between the experimental (hatched areas) and theoretical (points) dynamical emission in the Ar+Ni collisions at (a) 52, (b) 74, and (c) 95 MeV/nucleon.

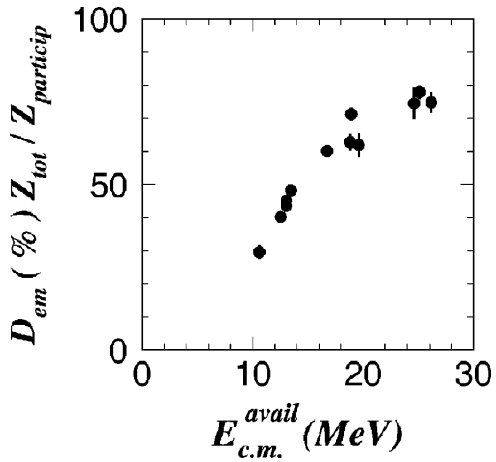

FIG. 4. Dynamical emission normalized to the participant charge as a function of the available center-of-mass energy for the 12 reactions of Table I in head-on collisions.

agreement is found between the calculation and the experiment at all three energies. As for the Xe+Sn and Ar+Ag systems, $D_{\rm em}$ saturates in central collisions and this behavior reduces to the most central collisions with increasing incident energy. The DE found in peripheral collisions at the three incident energies is almost identical.

The behavior of these three systems at different incident energies suggests that the geometry plays an increasingly important role with increasing incident energy. At 50 MeV/nucleon, the geometry is important for peripheral collisions. As the energy increases, geometrical effects increasingly affect the behavior of central collisions. At energy higher than 100 MeV/nucleon, the geometry becomes the key parameter, as found by the participant-spectator model [1].

Table I reports all 5 colliding systems studied in head-on collisions, which cover a large domain of asymmetry and total mass. Also, a large range of incident energies has been studied. By comparing the $D_{\rm em}$ values obtained for these different combinations of projectiles and targets at various energies, one finds that Ar+Ag at 50 MeV/nucleon gives the same amount of DE as Ag+Ar at the same incident energy per nucleon. Moreover, $D_{\rm em}$ is the same for the Ar+Al collisions at 41 MeV/nucleon and the Ar+Ag collisions at 50 MeV/nucleon, and these two reactions possess the same available energy per nucleon in the center of mass ($E_{\rm c.m.}^{\rm avail}=(E_{\rm P}/A_{\rm P})[A_{\rm P}A_{\rm T}/(A_{\rm P}+A_{\rm T})^2]=9.9$ MeV/nucleon). All these features suggest that the $E_{\rm c.m.}^{\rm avail}$ normalized to the participant mass is a relevant variable to classify all $D_{\rm em}$ results.

In Fig. 4, DE is plotted as a function of the $E_{\rm c.m.}^{\rm avail}$ normalized to the participant nucleons for all 12 system and energy combinations studied and extrapolated to head-on collisions ($b=0$ fm). Dynamical emission has been normalized to the participant charge $Z_{\rm particip}$, i.e., to the amount of charge being in the geometrical overlap of the target and the projectile [$D_{\rm em}(Z_{\rm tot}/Z_{\rm particip})$]. It can be seen that all 12 points behave coherently, displaying an asymptotic tendency towards 100% of DE as the incident energy increases beyond a few hundred MeV/nucleon.

As stated in the description of the model, our model is

sensitive to both the mean field and *NN* collisions. Thus, the reaction mechanism is the result of the interplay between these two physical quantities: Mean-field effects affect the whole system, whereas ''hard'' *NN* collisions are more localized in space. In particular, the Pauli principle greatly favors *NN* collisions involving one nucleon from the target and one from the projectile. This is due to their high relative momentum which allows them to explore the empty zone in the phase space. In this way, *NN* collisions create a highly excited zone in the overlapping region between the target and the projectile. The size of this zone will be more and more accurate as the incident energy increases since mean-field effects decrease.

In conclusion, a theoretical study of dynamical emission as a function of incident energy, impact parameter, system mass, and asymmetry has been carried out within the framework of the Landau-Vlasov model. It has been found that an increasing amount of matter is dynamically emitted as the $E_{\mathrm{c.m.}}^{\mathrm{avail}}$ increases. Dynamical emission increases with centrality of the reaction and saturates in central collisions. As the incident energy increases, DE increases and the global features tend to values expected from a simple geometrical model. Peripheral collisions follow the geometrical trend earlier than central collisions.

The above results suggest that DE is the bridge between the low-energy reaction mechanism (deep inelastic model) and the high-energy reaction mechanism (participant-spectator model). This transition occurs smoothly with increasing incident energy.

[1] G. D. Westfall, J. Gosset, P. J. Johansen, A. M. Poskanzer, W. G. Meyer, H. H. Gutbrod, A. Sandoval, and R. Stock, Phys. Rev. Lett. **37**, 1202 (1976).

[2] V. Métivier *et al.*, in *Proceedings of the XXXIII International Winter Meeting on Nuclear Physics* Bormio, Italy, 1995, edited by I. Iori (University of Milan Press, Milan, 1995), p. 255.

[3] J. Péter *et al.*, Nucl. Phys. **A593**, 95 (1995).

[4] J. Łukasik *et al.*, Phys. Rev. C **55**, 1906 (1997); E. Plagnol *et al.*, in *Proceedings of the International Nuclear Physics Conference*, Paris, 1998 [Nucl. Phys. A (to be published)].

[5] J. Toke *et al.*, Phys. Rev. Lett. **75**, 2920 (1995).

[6] B. Borderie *et al.*, Phys. Lett. B **205**, 25 (1988).

[7] E. Vient *et al.*, Nucl. Phys. **A571**, 588 (1994).

[8] J. G. Ma *et al.*, Phys. Lett. B **390**, 41 (1997).

[9] Ph. Eudes, Z. Basrak, and F. Sébille, Phys. Rev. C **56**, 2003 (1997); in *Proceedings of the XXXVI International Winter Meeting on Nuclear Physics*, Bormio, Italy, 1998, edited by I. Iori (University of Milan Press, Milan, 1998), p. 277.

[10] Z. Basrak, Ph. Eudes, P. Abgrall, F. Haddad, and F. Sébille, Nucl. Phys. **A624**, 472 (1997).

[11] T. Lefort *et al.*, Nucl. Phys. A (submitted).

[12] P. Pawloski, Phys. Rev. C **57**, 1771 (1998).

[13] C. P. Montoya *et al.*, Phys. Rev. Lett. **73**, 3070 (1994).

[14] J. F. Dempsey *et al.*, Phys. Rev. C **54**, 1710 (1996).

[15] Ph. Eudes and Z. Basrak, in *Proceedings of the International Nuclear Physics Conference* [4].

[16] D. Doré *et al.*, in *Proceedings of the XXXVI International Winter Meeting on Nuclear Physics* [9], p. 381.

[17] B. Remaud, C. Grégoire, F. Sébille, and P. Schuck, Nucl. Phys. **A488**, 423c (1988).

[18] J. Dechargé and D. Gogny, Phys. Rev. C **21**, 1568 (1980).

[19] J. Cugnon, A. Lejeune, and P. Grangé, Phys. Rev. C **35**, 861 (1987).

[20] V. de la Mota *et al.*, Phys. Rev. C **46**, 677 (1992).

[21] F. Haddad, F. Sébille, M. Farine, P. Schuck, V. de la Mota, and B. Jouault, Phys. Rev. C **52**, 2013 (1995).

[22] F. Haddad, J. B. Natowitz, B. Jouault, V. de la Mota, G. Royer, and F. Sébille, Phys. Rev. C **53**, 1437 (1996).

[23] M. Germain *et al.* (unpublished).